5-1997

Freezing Point Mobile Munitions Assessment Sytem: Thermal Chamber Redesign

Sara Gifford
Utah State University

Preston Harris
Utah State University

UtahState University
MERRILL-CAZIER LIBRARY

5-1997

Freezing Point Mobile Munitions Assessment Sytem: Thermal Chamber Redesign

Sara Gifford

Preston Harris

Footer Logo

FREEZING POINT MOBILE MUNITIONS ASSESSMENT SYTEM: THERMAL CHAMBER REDESIGN

By:

Sara Gifford
and Preston Harris

Thesis submitted in partial fulfillment
of the requirement for the degree

of

UNIVERSITY HONORS
WITH DEPARTMENTAL HONORS

IN

MECHANICAL AND AREOSPACE ENGINEERING

UTAH STATE UNIVERSITY
LOGAN, UT

1997

Table of Contents

1.0 Introduction

The Army is actively investigating non-intrusive methods to identify six chemical weapons agents. The chemical munitions in question are often found scattered across military bases and other facilities. These non-stockpile munitions are specifically targeted for identification using the mobile munitions assessment system. This program is being administered by the Idaho National Engineering Laboratory.

A research effort to determine the feasibility of identifying chemical agents through external freezing point measurement was conducted during the summer of 1996. The project demonstrated that the freezing point of test substances could be reliably inferred by external temperature measurement. There is every indication that freezing point determination would provide valuable complementary data to such procedures as gamma ray densitometry, x-ray crystallography, and other identification tests currently in use by the mobile munitions assessment system.

The Army invested approximately $21,000 to determine if freezing point identification is a viable method to non-intrusively identify chemical agents. This method has proven to be viable in determining the freezing point of water contained within steel shells. This is a large monetary investment for just a trivial piece of knowledge. An improved system model was developed as a senior design project at Utah State University. Tap water was the major test substance used for improvement verification.

1.1 Objectives

Design, build, and test an optimized thermal chamber for use in a mobile munitions assessment system to be used by the military that can non-intrusively identify chemical agents contained within a variety of chemical shells.

1.2 Requirements

The freezing point mobile munitions assessment system must satisfy six major requirements. It is necessary to impose these requirements on all components of the system,

including the redesigned thermal chamber. These requirements were developed by the military who instigated the initial research of a freezing point measurement system.

A. Test time

Test time is the most important constraint on the thermal chamber. The Army is interested in maintaining a maximum test time of 2 hours. The test time is to include set up and temperature measurement. Though, data analysis time is not included in any specific requirement from the military it is implied that the data collected can be quickly analyzed to render identification of chemical agents as soon as possible.

The thermal chamber must be designed such that the 2 hour test time is not exceeded. Initial testing revealed that heat removal rate plays a large role in freezing point identification. If the shell is cooled too quickly the freezing point will not be evident in the data. If the shell is cooled too slowly the test time limit will be violated. Optimal heat removal rates must be attainable by the thermal chamber using the recirculating cooler as the heat sink.

B. Accuracy

The freezing point measurement system must be highly accurate. The problems encountered by incorrect identification of chemical agents are great. The six chemical agents in question are rendered inactive by several processes. If a chemical agent is incorrectly identified it could be disastrous for the employees destroying the chemical rounds.

It should be noted that the freezing point mobile munitions assessment system does not need to identify each chemical agent. The freezing point identification method will be coupled with several other systems to identify each agent. But the freezing point method must be accurate in that it will identify or rule out an agent.

C. Non-intrusive Method

The chemical agents must be identified by a non-intrusive method. The chemical shell must remain intact throughout the test. Any intrusion into the shell would cause the agent to leak out and contaminate an area. Additionally, the test procedure must not in any way corrupt the strength of the shell. The shell must be shipped to disposal facilities after identification. Shell failure during shipping could be catastrophic. Air born chemical agents could severely incapacitate or kill a person with a small dose, such as several breathes. The

seals and fuses of the ordnance must not be compromised in any way. This requirement restricts thermocouple placement to the outside of the chemical weapons shells. Additionally, the thermal chamber must accommodate such measurement techniques.

The phase change measurement may occur with thermocouples or with heat flux gauges. These measurement devises must be safely attached to the chemical weapons shell. The Army has specified that the previous technique, grinding a smooth surface on the shell then welding a thermocouple to it, is unacceptable. They fear, with good reason, that this is an unsafe activity with a live chemical weapon shell. An alternative, safe technique must be developed.

D. Two Person Operation

The freezing point identification system must be fully operational with two to three people staffing the mobile munitions identification system. The implication for the thermal chamber are quite clear: the shells must be easily inserted and removed from the thermal chamber with minimal personnel risk (i.e. back problems). This requirement becomes more stringent when the maximum shell weight of 100 lb is considered.

E. Size

The thermal chamber must accommodate testing of 105 mm, 155 mm, and 4.2 in mortar shells. These shells represent a large size range. The largest shell is the 155 mm. Its dimensions are 15.5 cm in diameter and 61 cm in length. The chamber must also accurately and effectively be used in testing of smaller shells specifically the 4.2 in mortar shell. Presently, a complete 105 mm shell is not available for testing, however, it should be considered in the design of the thermal chamber.

F. Environmental Conditions

The freezing point mobile munitions assessment system will be subjected to the following non-operating environment:

> Temperature: -25°F to 110°F
>
> Humidity: 0 to 100% non-condensing

The operating environment of the thermal chamber is limited to:

> Temperature: 65°F to 85°F

G. Durability and Maintainability

The chamber must withstand excessive fatigue resulting from setup, use, and relocation. It must be durable. If replacement parts are needed they must be obtainable at local stores or with minimal special order delays.

2.0 Recirculating Cooler System Analysis

The recirculating cooler system was analyzed to determine the areas that most needed improvement to satisfy the overall project requirement of a two hour test time. The recirculating cooler has the ability to produce 880 W of cooling at -60°C. Several tests revealed that the temperature drop across the thermal chamber was less than 0.5°C during the freezing of a 155 mm shell. It was expected that the temperature of the heat transfer fluid would drop much more across the thermal chamber. This test focused our efforts on improving the thermal chamber.

A more rigorous calculation to verify that the thermal chamber was indeed increasing the test time was made from a test on the 4.2 in mortar shell. Comparing the cooling rate from the temperature time plot, the heat removal rate can be estimated. The estimated heat removal rate is 34 W. This heat removal rate represents an efficiency than less 5% of the capacity of the recirculating cooler. The thermal chamber was identified as the system component that significantly increased the length of tests from this calculation.

Two distinct areas of the thermal chamber have been identified as significant contributors to the low heat removal rate. Conduction from the heat transfer fluid in the copper coils to the interior of the chamber is low. Convection heat transfer through the air space to the chemical weapon shell was lacking. The specific problem in each of these areas is further discussed in this section. Potential improvements will be detailed. The improvement method selection is made. The results of these improvements are discussed in test results of the report.

The heat transfer fluid is delivered to the thermal chamber via a single pass copper tube loop. The copper tube makes approximately 18 loops around the thermal chamber then returns to the recirculating cooler to be cooled and circulated again. In each test, the recirculating cooler was set to -60°C, its lowest possible temperature setting. The heat from

the high temperature (initially at ~20°C) test fluid must be transferred through the 1/2in steel shell wall, a 1 to 2in air space, the 1/8th inch PVC wall, and the copper tubing to the low temperature (-60°C) heat transfer fluid.

The heat transfer from the test fluid to the heat transfer fluid can be modeled as one dimensional thermal circuit because the thermal chamber is radially symmetric. The thermal circuit is shown in figure 1. For this model , the heat removal rate is only dependent on the thermal resistance because the temperature of the test fluid and heat transfer fluid are initially constant. A high heat removal rate will develop if the thermal resistance is low.
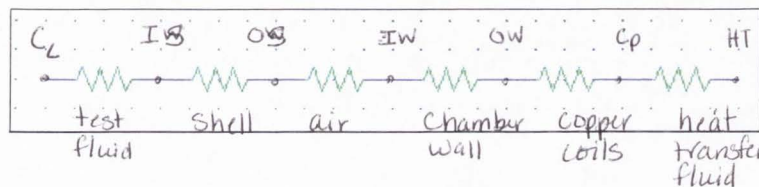
Figure 1. Thermal circuit analogy for the thermal chamber. The resistance of the air and chamber wall can be reduced to increase the heat transferred to the shell.

It is clear that the thermal resistance must be reduced to increase the heat transfer rate and reduce test lengths. The thermal resistance of the test fluid is constant. The distance from the centerline to the shell wall and the thermal conductivity of the test fluid can not be changed. The resistance of the shell is also constant. The shell thickness can not be reduced by grinding it down before testing. The thermal resistance of the "copper tube contact" is relatively constant. The heat transfer fluid is most efficiently transported to the thermal chamber by via a tubing loop. The only areas that can be significantly modified to increase

the heat transfer rate of the thermal chamber are the interior chamber wall and the air in the air space.

2.1 Conduction through the Interior Chamber Wall

Heat must be conducted through the interior chamber wall. The thermal resistance for this component of the thermal chamber can be expressed in term of the thickness of the material, L, the thermal conductivity coefficient, k, and the surface area, A.

$$R_{wall} = \frac{L}{kA}$$

The resistance of the thermal chamber interior wall is large because PVC has a low coefficient of thermal conductivity (0.2W/mK). The thermal resistance of the interior wall can be reduced in two ways. The thickness of the PVC can be decreased or the material can be changed to one with a larger coefficient of thermal conductivity. Either of these two options will result in a lower thermal resistance to heat transfer through the interior chamber wall. The heat transfer area is left as a constant because the area currently in use is convenient and satisfies several other requirements. The heat transfer rate will increase when the thermal resistance is decreased.

2.2 Convection through the Interior Air Space

The air gap is an important feature of the thermal chamber. It prevents an exceedingly strong thermal link from forming between the chemical weapons shell and the heat sink. A thermal link that is too strong would cause the external shell temperature to rapidly drop to the temperature of the heat sink. The steel shell wall will conduct along its length much faster than it will conduct to the test fluid. The freezing point temperature of the test fluid could not be detected. The external shell temperature measurements would be "smeared". The shell rests on insulating styrofoam pads to maintain an air gap with the chamber wall.

A verification test was performed to quantify the effect of the stagnant air in the gap. The 4.2in mortar shell was filled with water and placed in the thermal chamber. Several thermocouples were attached to the shell. One thermocouple was placed near the center of the air gap. The temperature time plot is shown in figure 7. The air temperature follows the external shell temperature trend by a -15°C offset. In order for a high heat transfer rate to be achieved the temperature of the air in the gap must be close to the heat sink temperature (-60°C). The air does not reach 0°C for nearly half an hour. When freezing of the test fluid is detected the air temperature is -15°C.

Stagnate air tends to insulate more than first anticipated. This was not recognized as a design factor until after the thermal chamber had been constructed. The air gap can be used as a heat transfer mechanism if the air is moving. Air blowing over a cold surface (the chamber wall) can remove heat from a warm surface (the shell). Dr. John Morrison and Dr. Randy Clarksean confirmed that the air could be moved around inside the thermal chamber with small fans. This air movement would result in a higher heat transfer rate.

In order to achieve a higher convective heat transfer coefficient, the insulating effects of the air gap must be reduced. The initial plan is place a fan at each end of the thermal chamber. These fans will provide the necessary air movement to implement convection heat transfer. A simple numerical model, to be explained later, will be used to determine an optimum convection heat transfer coefficient. This model will also be employed to determine the convection heat transfer coefficient produced by various shell and fan combinations. Fluent will be used to model the air currents produced by a fan in the thermal shell.

3.0 Thermal Chamber Redesign

The thermal chamber was selected for redesign based on the recirculating system analysis. The component(s) that most inhibit a high heat transfer rate are to be incorporated into the redesigned thermal chamber. The overall project requirements and objectives as well as cost are to be considered as design factors.

3.1 Specifications

The previous construction of the thermal chamber was suspect for the 34 W of cooling out of the 880 W possible. Upon investigation the materials chosen were determined to have poor thermodynamic properties. The inner chamber wall was made of PVC pipe which was found to have a thermal conductivity of only 0.2 W/mK.

To make the thermal chamber more efficient, materials with a high thermal conductivity were selected for the inner wall. The bases for selection was availability, cost, density, and yield strength of the material. Using these criteria the possible materials for use were copper and aluminum Both materials were in stock at Utah State University technical services.

The material properties for copper are a thermal conductivity of 400 W/mK, a density of 8.94 g/cm^3 and a yield strength of 69 MPa. While the mechanical properties of 2024 T6 aluminum has a thermal conductivity of 177 W/mK. Aluminum has a density of 2.8 g/cm^3 and a yield strength of 97 MPa.

To produce the thermal chamber wall out of copper the quoted cost was \$400 while aluminum was \$200. The final decision for the choice of the material was based on the calculation using the maximum possible heat transfer for each material at three available thickness, 1/8", ¼", 3/4". For all materials and wall thicknesses it was calculated that the possible heat transfer from the recirculating cooler would be restricted by the material (see appendix). Aluminum was chosen for the inner wall because it was less expensive and could still provide a high heat transfer rate.

The next part of the thermal chamber that was considered a problem was the coils. The coils were placed with a 2" gap between the coils, this causes cold spots separated by a large temperature gradient caused by the poor thermal conductivity of the PVC. The decision concerning the coils was in order to eliminate the cold spots, the coils needed to be close together so we chose the new coils to be closed packed.

To facilitate conduction into the chamber , the next wall needed to be thermally resistant. Two materials were chosen mylar and expanding foam. The mylar would perform two functions, reflect the cold into the chamber and act as a barrier so the

expanding foam didn't get underneath the coils and insulate the inner chamber wall from the coils. The expanding foam chosen was a isocyonate - polyoyl two part foam. This two part foam was ordered because it has a R value of about ~7/inch while the canned expanding foam is abut ~5/inch. The deciding factor was the two part foam produces an exothermic reaction that causes expansion thus not needing air to expand. The canned foam needed air to expand which meant in the annulus condition of the thermal chamber the center section never expanded to full insulating value because of a lack of air.

Since the outer wall is not critical PVC will again be selected because of its durability and availability.

Besides the materials aspect, the dimensionally of the chamber needed to be redesigned. One problem of the first chamber was the 155mm shell could barely fit. The shells are ~24 inches while the thermal chamber is 27 inches. To allow room for fans and the shells the thermal chamber was designed to 4 feet long the diameter was going to keep the insulating effect of the air down the tube was resized to 8 1/4" diameter for ease of manufacturing.

4.0 Modeling

Two computer models were employed to guide the development of the thermal chamber. The convection heat transfer was modeled using a FORTRAN program based on the explicit enthalpy method. This model can be used to estimate the convection heat transfer coefficient. The commercial fluid mechanics program Fluent was employed to determine the air currents around a shell induced by given fan configuration. The program can also provide estimates into the test length. These models were invaluable in the design of the thermal chamber.

4.1 Enthalpy Method to Model Test Fluid Phase Change

The enthalpy method is used to model phase change problems. The phase change problem is formulated by a single equation written in terms of enthalpy. It can accurately

model phase changes that occur over a temperature range as well as those that occur at a discrete temperature. The enthalpy method is employed to estimate the convection coefficient induced by a fan inside the thermal chamber. The temperature time plot produced in a test can be compared to a plot developed by the enthalpy method for a given convection coefficient. The theory and algorithm used in this model are further developed in appendix c.

The explicit enthalpy method is a good method to estimate the convection coefficient induced by a fan in the thermal chamber. However, it does not perfectly model the actual thermal chamber and chemical weapons shell during freezing. No attempt was made to include the burster tube in this model because only the 4.2in mortar shell contains an actual burster tube. A simple modification could be made to model the burster tube for any shell provided the shell dimensions were accurately known. The one dimensional approximation suggests that the convection coefficient is uniform around the shell. This is not the case. Flow velocity test indicate that the air speed around a shell is fastest near the fan and slowest far away from the fan. Additionally, the installation over the thermocouples and hose clamps prevent a uniform convection coefficient by disrupting the flow. The explicit enthalpy method makes no attempt to model the convection and flow of the test fluid during cool down. Dr. Randy Clarksean developed extensive finite element models to characterize the internal flow. This model assumes that internal convection is uniform affecting the shell temperature evenly. Nevertheless, the explicit enthalpy method is a useful tool to estimate the uniform convection coefficient induced by a fan inside the thermal chamber.

The original plan was to estimate the convection coefficient induced by a fan inside the thermal chamber. Unfortunately, the redesigned thermal chamber was never built. The comparison to actual testing was not conducted. The airflow rate can not be estimated for the original thermal chamber. For example, a fan with a large capacity may not necessarily produce a higher air flow rate because of the restrictions on the air flow within the chamber. It was difficult to determine how an optimum convection coefficient could be attained even if one had been determined. The tasks of this design project were focused on reducing the test time below the 2 hour limit and developing a feasible thermocouple attachment technique. Therefore, it was decided that time would be better spent on achieving these

goals than on this analysis technique. In fact, the test time was not reduced until the last week of the project. At which time, the focus of the project was the report and analysis of these lower test times.

4.2 Fan Flow Analysis: Fluent

From discussions we decided to use one fan, approximately the same diameter as the inside of the thermal chamber, at the front of the chamber. This was the first configuration to be modeled on fluent. The model showed that the large fan was not applying any significant increase in air velocity because it was only circulating the air within the immediate extremities of the fan as seen in figure 2. These results were confirmed on the experimental setup when the end closest to the chamber behind the shell the air flow velocity was 950 ft/min. When the cover was placed on behind the fan, the velocity fell to a measured 0 ft/min.

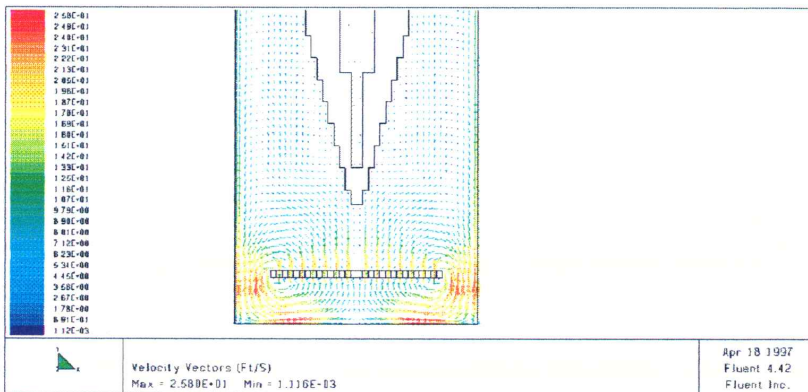Figure 2. Fluent model of one fan in the thermal chamber. This model shows restricted flow

From the model it was decided we could try putting a fan at both ends. This model showed we could have a significant air velocity across the surface refer to figure 3. The only problem was there is on confirmation, the fans purchased were significantly below those modeled. The fans that were used produced no measurable flow across the shell.

Temperature (R)
Max = 4.592E+02   Min = 3.837E+02   Time = 1.800E+03

Apr 25 1997
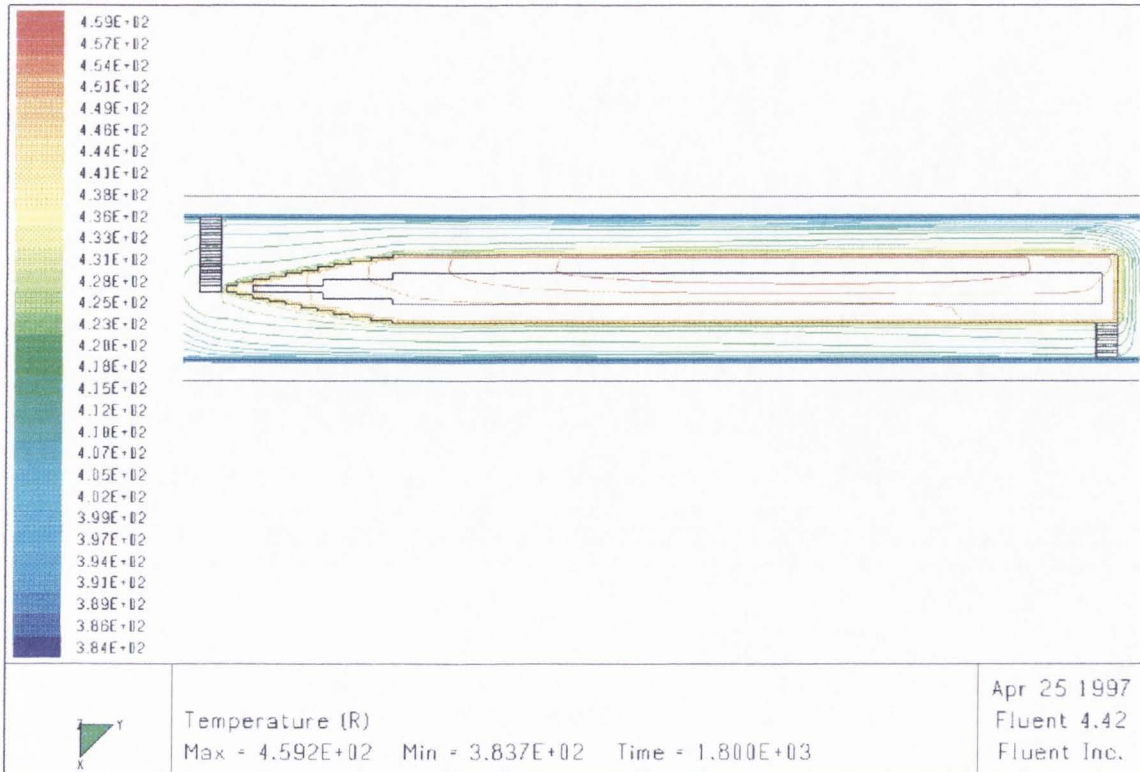Fluent 4.42
Fluent Inc.

Figure 3. Fluent model showing the use of two fans and their effect on air

Another model was developed using one fan on top of the shell. This model showed favorable air flow around the shell as seen in figure 4.

Temperature (R)
Max = 5.330E+02   Min = 3.837E+02   Time = 3.600E+03
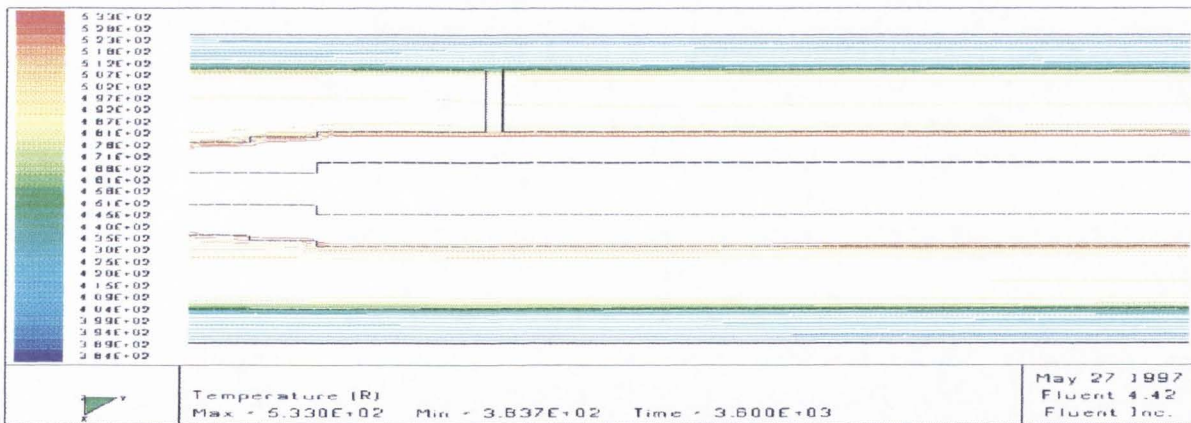
May 27 1997
Fluent 4.42
Fluent Inc.

Figure 4. Fluent model with one fan on top.

The models with the fans and without were run using the thermoconductivity of PVC and Aluminum 2024 T6 to compare the test times. The two different models show that the higher conductivity may decrease our test times by at least a half.

The modeled conditions being used to check the tests were the walls have a thermal conductivity, the time temperature ramp function used by the circulating cooler was applied to the wall and a 155 mm shell was used for the dimensions of the shell in the model.

5.0 Thermocouple Attachment Technique

During previous research it was discovered that merely placing the thermocouples on the shell resulted in a 2 or 8° Celsius temperature differences. To evaluate this a thermocouple test was conducted (see below for results).

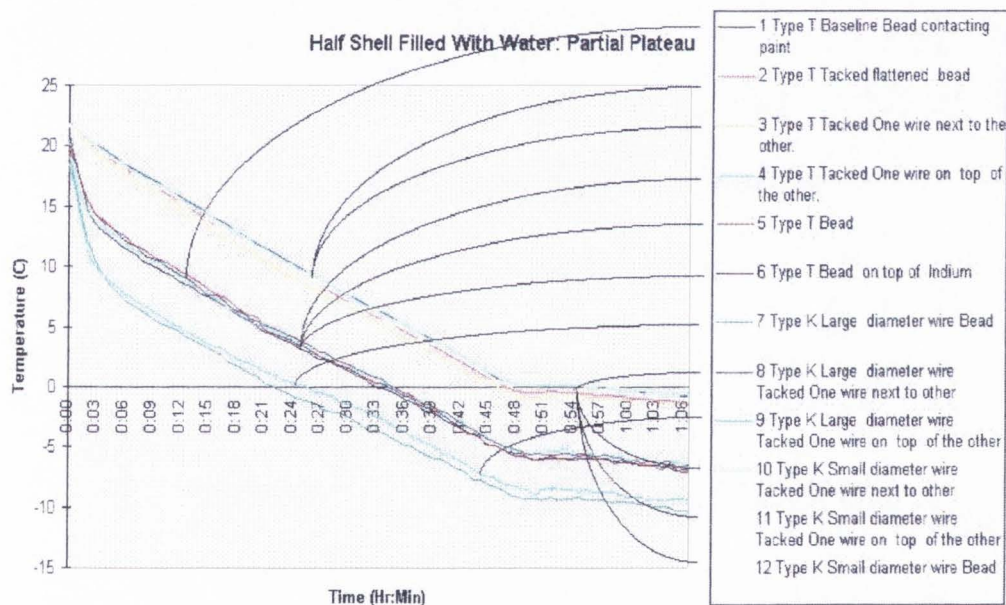

Figure 5. Thermocouple test to experimentally determine accurate thermocouple attachment techniques and appropriate thermocouple types and sizes.

From graph we looked for a common variable among those thermocouples around the expected temperature. The only test scenario that possessed common characteristics were the welded thermocouples, with the leads side by side, all measured temperatures

around the expected temperature. We decided to then weld the thermocouples. Welding purposed some concern for mounting the thermocouples to the live shells. Tests were performed to evaluate methods of mounting the thermocouples for best accuracy. The most consistently accurate reading was for welding the leads side by side as seen in figure 5. This is confirmed theoretically in the book <u>Manual on the Use of Thermocouples in Temperature Measurement</u>. Welding the thermocouples was fine for the laboratory and inert materials , but could be problematic for a shell in the field. So a new safe and accurate method of temperature measurement needed to be determined. The previous thermocouple test showed one possibility, a thin type K thermocouple refer to figure 5.

To test the thin thermocouple theory, five 36 AWG type K thermocouple wires were ordered. Two thin wired thermocouples were then tested and compared against the welded thermocouples. They reported virtually the same temperature, the maximum temperature differences between the thermocouple was 0.2^0 Celsius (see figure 6).

Thermocouple Test
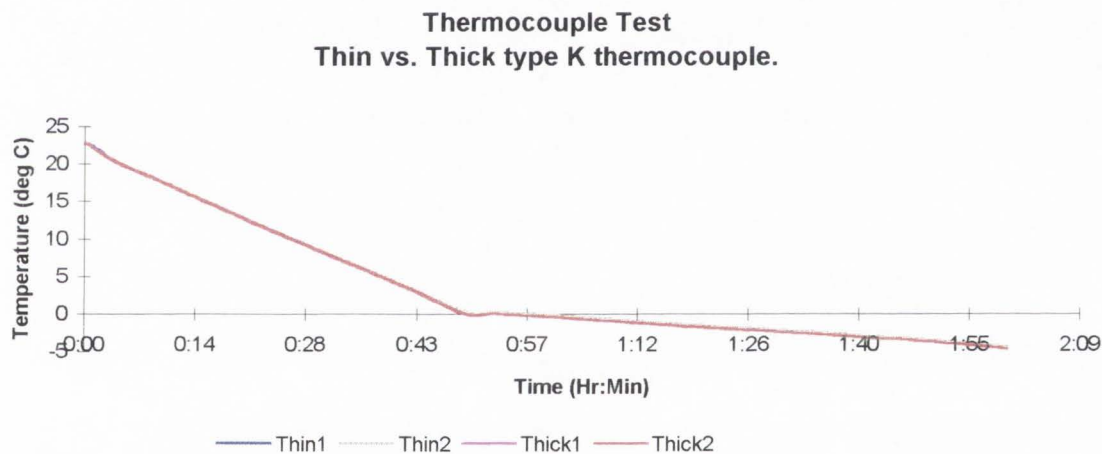**Thin vs. Thick type K thermocouple.**

Figure 6. Thermocouple test: comparison of thick and thin type K thermocouples.

From the test it was determined that if the shell could be sanded then a thin diameter thermocouple could be mounted using an adhesive backed felt or cork tabs to hold the thermocouples in place.

6.0 Test Results

The most significant test results are presented in this section. Tests were conducted using the original thermal chamber. The 4.2 in mortar shell was used because it provided ample space for fans to be inserted into the chamber. In general, the test fluid was water. Water was chosen because of the distinct slope change in the temperature time plot. The focus of this series of tests was explore the results of increasing the convection on the interior of the shell. The temperature in the air gap is also examined to provide an idea of the effect of the convection coefficient changes. A heat flux sensor is utilized as an alternate phase change detector.

Test 1: 5/26/97

This test serves as the base test for the 4.2 in mortar shell filled with 2 L of water. The 4.2 in mortar shell was placed in the thermal chamber. The recirculating cooler was started. The air in the air gap was stagnant. The shell was instrumented with 3 type K thermocouples and a heat flux sensor. Two thermocouples were attached to the surface of the shell using the felt tab method. The air temperature was measured with a type K thermocouple. The heat flux sensor has a thermocouple in its thin film. This thermocouple is designated as "Thin Film".

The phase change was seen in just under 2 h.

Base Test: 4.2 in Mortar Shell
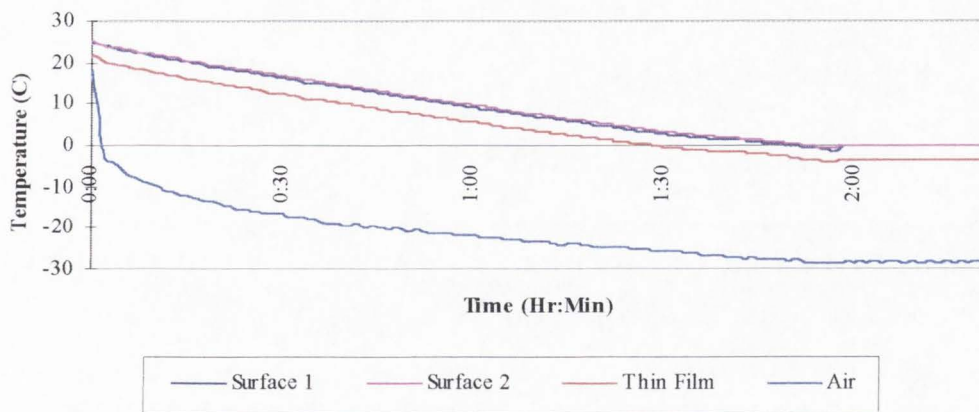
Figure 7. The base test of the 4.2 in mortar shell filled with 2 L of tap water. The test time is one hour and fifty minutes.

Comparison of Heat Flux to Surface Temperature Over Time
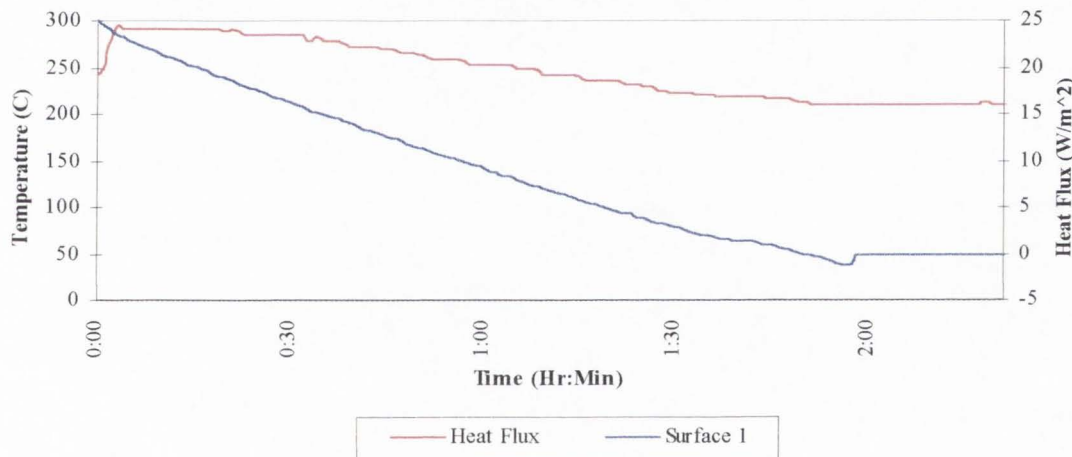
Figure 8. For the base test of the 4.2 in mortar shell, the heat flux was compared to the temperature over time. Upon freezing, the heat flux curve has plateau similar to the temperature curve plateau.

Test 2: 5/21/97

This is a test of the 4.2 in mortar shell filled with 2 L of water. An 18 VDC fan was used to induce a higher convection coefficient around the shell throughout the test. The fan was placed near the nose of the shell. This fan can move 115 cfm. The flow rate around the shell measured at the opposite end of the chamber was 950 fpm with free flow through the chamber. However, when the end closures were placed on the thermal chamber the air

speed was negligible. The shell was instrumented with 3 type K thermocouples and a heat flux sensor. An additional type K thermocouple was placed in the air gap near the shell but away from the fan exit.

Complete Freeze of 4.2 in Mortar Shell:
18 VDC Fan

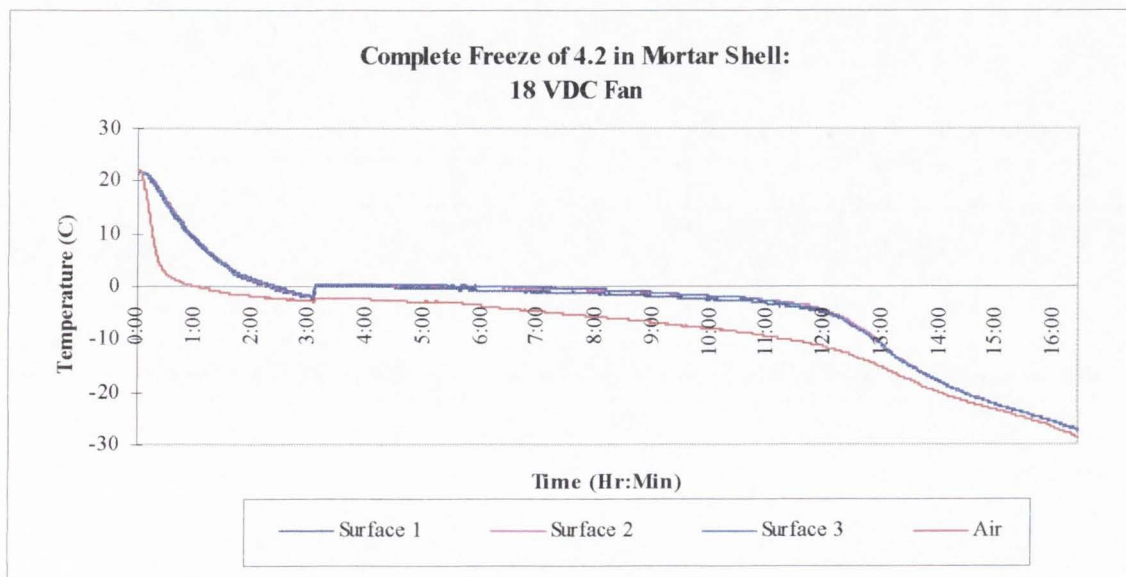Figure 9. The 4.2 in mortar shell was completely frozen in the original thermal chamber. The 18 VDC fan was used to induce an air current around the shell. Warm air was pulled into the thermal chamber resulting in a test time of 3 hours.

The freezing point was detected at approximately -2.2°C by the surface thermocouples in just over 3 h. The observed test time was extended by almost 1 h over a stagnate air test. This is a result of the pressure differences produced by the fan. Behind the fan a low pressure area developed. A high pressure area developed in front of the fan. The low pressure area pulled warm air from outside the thermal chamber inside. The warm air was circulated half way down the length of the shell. The warm air reduced the heat transfer from the shell because initially the shell and air were approximately the same temperature. The test time was further lengthened by freezing the moisture in the air. The warm air contained water vapor that condensed when it was cooled below its freezing point. The recirculating cooler system must first remove heat from the air and freeze the water vapor before heat can be removed from the shell.

Initially, the air temperature is influenced more by the temperature of the cooling coils. It takes about 30 min for the coils to reach their minimum temperature of -60°C.

During this time, heat is removed from the air and the temperature drops almost linearly with respect to time. The linear decreasing air temperature gives way to a parabolic trend once the coils have reached their minimum temperature. At this point, more heat is transferred to the air from the shell than is removed from the air to the coils. The air temperature follows the shell surface temperature.

By the time the test fluid changes phase, the air temperature is slightly lower than the shell surface temperature. The air temperature thermocouple records the same distinctive temperature dip. The temperature dip indicating a phase change is shown in figure 10. The air temperature a the phase change is -2.8°C while the shell surface is -2.2°C. This suggests that it may not be necessary to instrument the shell surface. It may only be necessary to measure the air temperature near the shell but out of the path of air flow. The air temperature continues to follow the surface temperature through the supercooling of the test fluid.

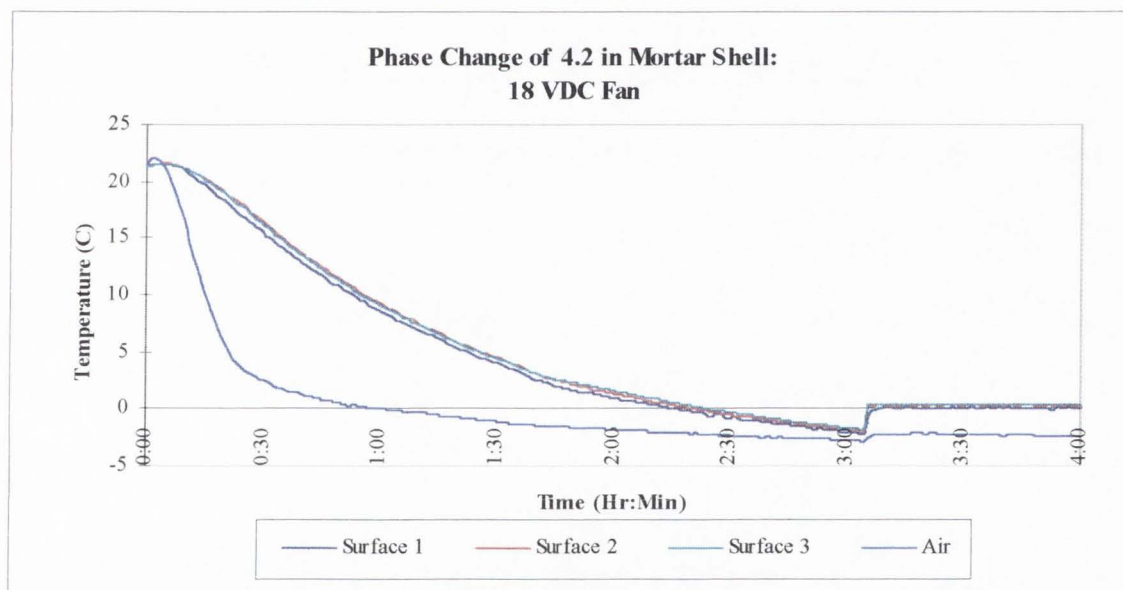Figure 10. The temperature time curve is focused about the phase change point. The air temperature displays the temperature jump which is characteristic of freezing water.

This test suggests three important concepts concerning increased air flow in the air gap. First, the thermal chamber must not be vulnerable to warm air intake. Warm air intake can be prevented by sealing the thermal chamber. Blocking possible warm air intake paths

prevents warm air from entering the chamber. Additionally, if the pressure inside the thermal chamber is kept constant by placing two fans of the same capacity at opposite ends of the thermal chamber warm air will enter the thermal chamber as easily. A combination of both of these solutions is the best approach. Second, air conduction can only have a positive effect on test times if the air temperature is less than the shell surface temperature. If the convective heat transfer occurs between warm air and the chemical munitions shell the test time can be significantly increased. Third, the freezing point of a test fluid can be discerned if significant air conduction is present. This fact is important to know. If convective heat transfer "smeared" the test fluid freezing point detection then this method of reducing the test time must be abandoned.

The heat flux should increase when the test fluid begins to change from the liquid to solid phase. A plot of the heat flux over time would provide a secondary method to identifying the phase change of the test fluid. Potentially, a characteristic plot could be developed for each test fluid. It may still be necessary to measure the shell surface temperature to identify the substance contained inside the shell.

In order to test this theory, a thin film heat flux sensor was attached to the 4.2 in mortar shell using teflon tape. This sensor was designed to accurately measure the heat transfer through any type of material. It has a sensitivity of $1.05 \ \mu V/W/m^2$. The heat flux sensor was not permanently attached to the shell. The sensor location can be changed to determine the optimum placement location. This choice would induce some errors in the measurements. They would not be as exact as if the sensor was permanently attached to the shell. However, the general trend in the heat flux plot should still accurately denote a slope change upon freezing.

The heat flux and surface temperature with respect to time are compared in figure 11. The heat flux has four notable slope changes. The first slope change occurs when the temperature of the air surrounding the shell begins to drop. Initially, the temperature shell was slightly below the temperature of the air. Heat was flowing from the air to the shell. When the air temperature began to decrease the heat flux also began to drop. The decreasing heat flux continued until the test fluid began to freeze. For water, the temperature increases slightly upon freezing. This temperature increase lead to a higher heat

flux. The heat flux remained relatively constant at 58 W/m^2. The heat flux started to increase when the interior thermal resistance of the shell dropped. The interior thermal resistance decreased because ice has a higher thermal conductivity than water. This change in thermal conductivity causes the interior thermal resistance to decrease. Therefore, the heat flux began to increase. The increasing heat flux continued until the test fluid was completely frozen and began to supercool. Upon supercooling, the heat flux decreased.
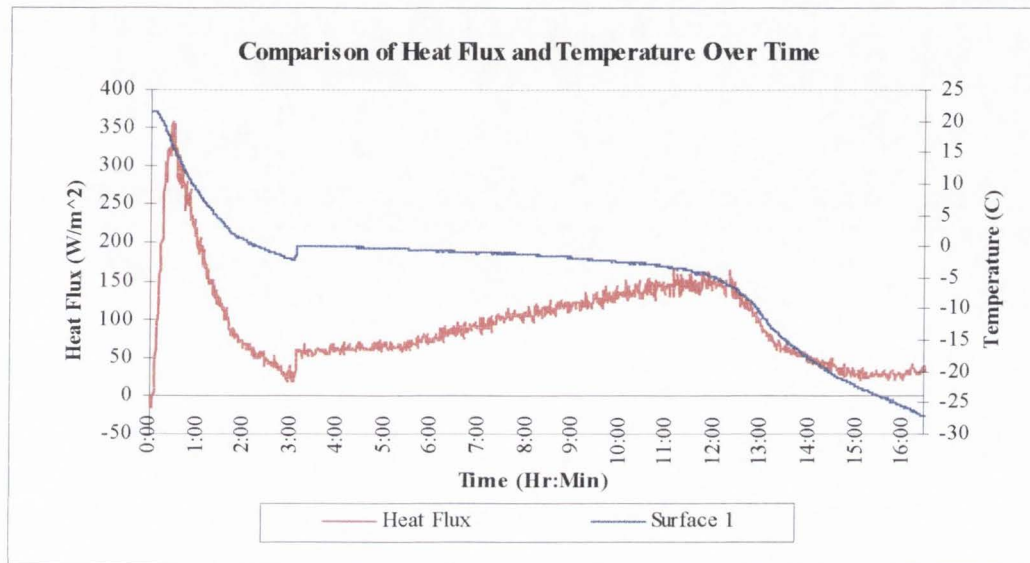
Figure 11. The heat flux curve is compared to the temperature curve for the complete freeze of the 4.2 in mortar shell. The heat flux curve registers the initiation of freezing and the supercooling of the water.

Even though, this test did not produce the overall desired result of significantly reducing the test time it did provide several pieces of valuable information. The shell surface thermocouples indicate that the pressure must be relatively constant inside the thermal chamber and the thermal chamber must be air tight to decrease the test time. The freezing point can be determined by external instrumentation if convection is a primary form of heat transfer from the shell. A heat flux gauge also indicates the occurrence of a phase change. The freezing point can be accurately determined by measuring the air temperature near the surface of the shell. This information was used to develop other tests.

Test 3: 5-24-97

This test was designed to test the theory that warm air intake increased the test time. The set up is similar to the previous test. The 4.2 in mortar shell was filled with 2

L of water and placed in the original thermal chamber. The 18 VDC fan was replaced with two 27.5 cfm muffle fans. By using two fans the pressure difference would not be as significant as with the large single fan. The fans were placed at the center of the chamber. The air flow was directly over the midsection of the shell. The shell was instrumented with 3 type K thermocouples on the surface and a heat flux sensor. A thermocouple was placed in the air gap directly in the path of the air from the fans. The shell was not placed in the thermal chamber until the coiling coils had reached their minimum temperature of -60°C.

The original thermal chamber was sealed from the surrounding warm air with weather stripping and new end closures. Weather stripping that was air and moisture tight and 0.75" thick was used to seal the chamber. Three layers were used. The new, tighter fitting styrofoam end plates butted up to a layer of the weather stripping. A layer was placed on the edge of each end plate. Finally, the outside of the end plate was sealed with the weather stripping.

Figure 12 is the temperature time plot of the resulting test. A slope break in the temperature time plot occurs at 2°C in 40 min. A temperature plateau occurs at -0.2°C in just over 1 h. This is an encouraging result because the freezing point is detected in well under 2 h. The air temperature is below the phase change temperature for water when the shell is inserted in the thermal chamber. However, a distinct slope break is still seen in this temperature time curve. The thermocouple marked "thin film" is attached to the thin film of the heat flux sensor. It is not permanently attached the shell. This thermocouple approximately measures the air temperature near the shell out of the influence of the fans. The temperature time plot displays a slope break at -5°C. This thermocouple shows that the air temperature near the shell but out of the direct influence of the fans can indicate the phase change temperature.

4.2 in Mortar Shell Under Two Muffle Fans
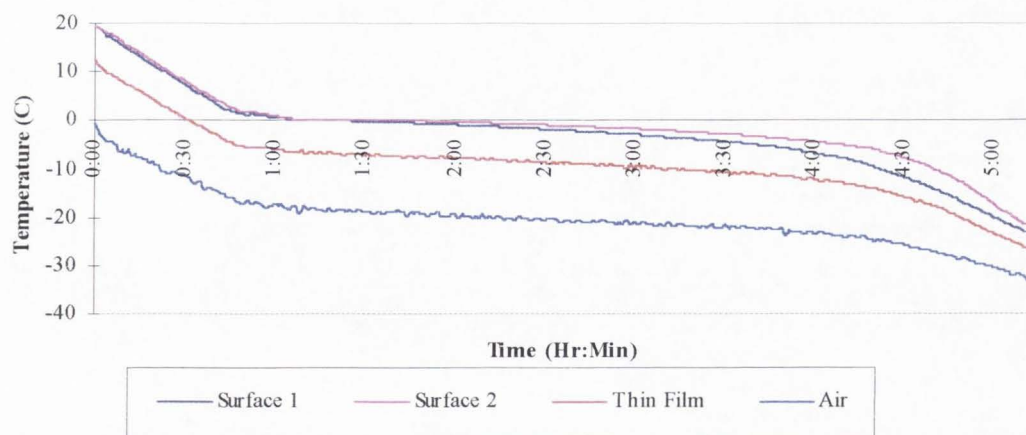
Figure 12. The 4.2 in mortar shell was completely frozen in the original thermal chamber. The thermal chamber was sealed with weather-stripping and styrofoam end caps. Two muffle fans were used to circulate the air around the shell. The test time was reduced to 1 hour.

The heat flux is compared to the temperature over the time length of the test in figure 13. The heat flux plot is quite jumpy this is because the sensor was loosely attached to the shell with teflon tape. The heat flux curve was fit with a trend line. The trendline shows the heat flux remains relatively constant throughout the liquid to solid phase change. When the solid begins to supercool the heat flux drops off rapidly.

Comparison of Temperature and Heat Flux
for the 4.2 in Mortar Shell
Under Two Muffle Fans

Figure 13. The heat flux curve is compared to the temperature curve. A polynomial curve fit is applied to the heat flux curve. The heat flux curve and the temperature curve plateau at the initial liquid to solid phase change.

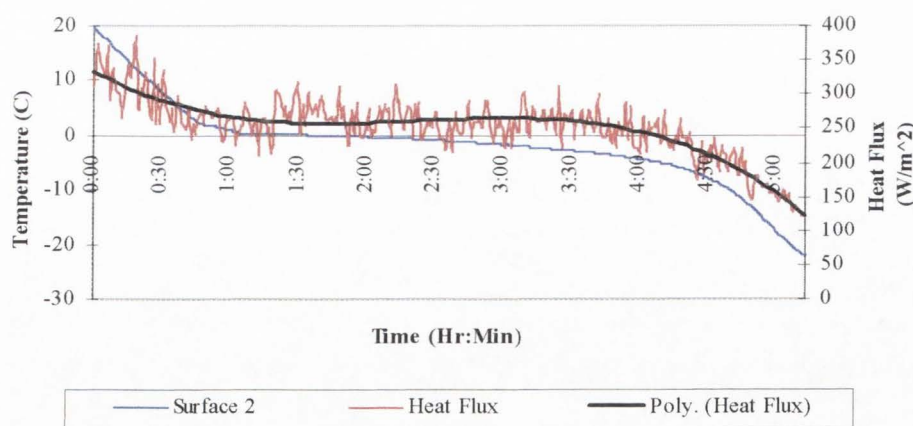This test showed that the test time can be significantly reduced by sealing the thermal chamber better. The phase change was detected in 1 h by the thermocouples and the heat flux sensor. The phase change temperature was correctly measured at 0°C.

Test 4: 5/28/97

This test is same as the second test. However, it was performed in the better sealed thermal chamber. The test results suggest that the long test time was induced by warm air pulled into the chamber. Figure * is the temperature time plot for this test. The phase change for water is detected just after one hour into the test. The curve break is distinct. The air temperature is -6°C. The heat flux sensor thermocouple reads -3.6°C. The surface thermocouples are at -0.6°C. This test indicates that the test time can be significantly reduced by using a fan to create convection heat transfer within the chamber. The phase change can still be detected under such circumstances.
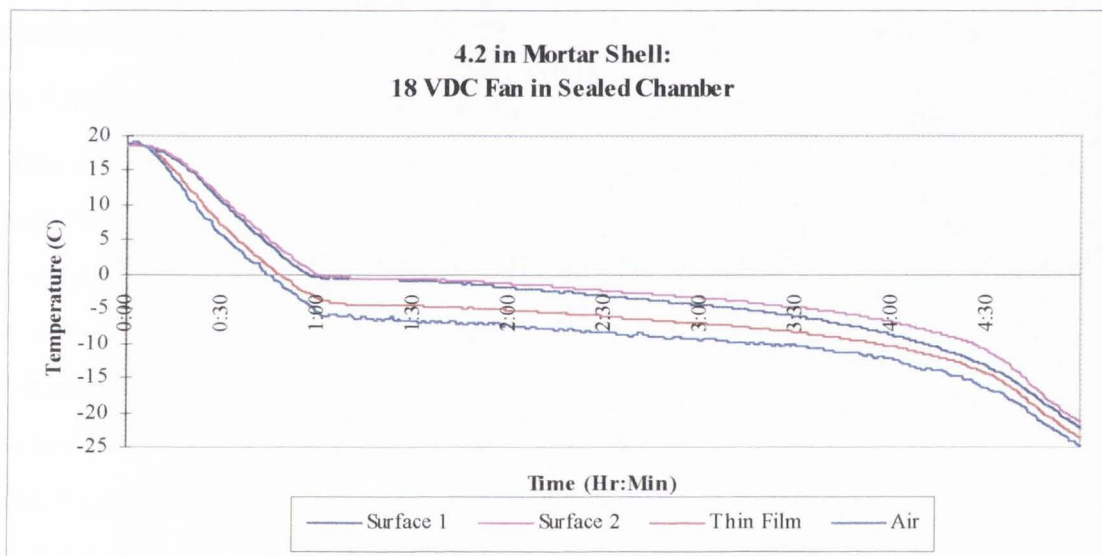

Figure 14. The 18 VDC fan is used to circulate air around the 4.2 in mortar shell. The shell is placed in the original sealed thermal chamber. The test time is reduce to 1 hour.

Figure 15 is the comparison of the heat flux to the temperature over time. The heat flux has a distinct slope break at the phase change time.
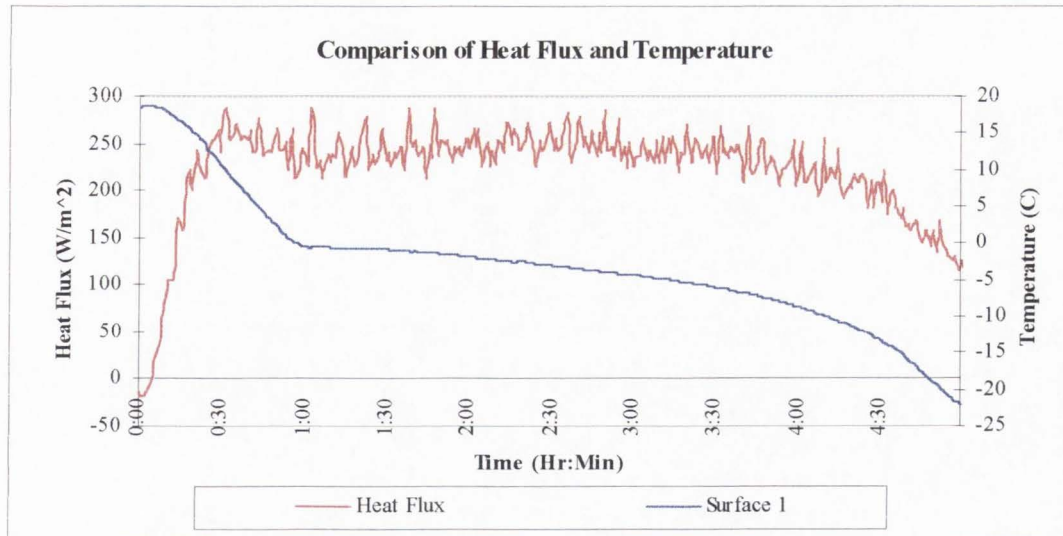
Figure 15. A plot of heat flux and surface temperature verses time.

7.0 Conclusion

7.1 Sara Gifford's Conclusions

This senior project provided an opportunity for design as well as research. The design portion of the project focused on analyzing the recirculating cooler system to achieve a reduction in test length. The analysis of the recirculating cooler system quickly focused the improvements to the thermal chamber. The ideas developed in the redesign of the thermal chamber lead to an opportunity for testing and research. Through research, both in literature and experiments, a reduction in test time was achieved. Research conducted during this project provides evidence that welding is not necessary to measure accurate shell surface temperatures.

The recirculating cooler analysis reveals that the thermal resistance of the thermal chamber produces long test times. The thermal resistance must be reduced in order to achieve shorter test times. Reducing the thermal resistances of the air gap and the interior wall are of greatest concern. The conduction coefficient of the thermal chamber wall material was increased. The higher conduction coefficient would allow heat to leave the shell at a higher rate. The thermal resistance is reduced by increasing the conduction coefficient. The air gap presented a completely different problem. The air gap is necessary to prevent a strong thermal link between the shell and the interior wall. The air surrounding

the shell was circulate around the shell with various fan configurations. Circulating the air around the shell reduced the thermal resistance by increasing the convection coefficient of the air.

The thermal chamber was redesigned. The materials and dimensions are specified. The thermal chamber was not constructed due to a budgetary crisis. The redesigned thermal chamber would have allowed testing to be conducted on the 155 mm shell. Instead testing was conducted in the original thermal chamber with the 4.2 in mortar shell. These tests revealed that the test time below the 2 hour limit can be achieved by circulating the air around the shell. To achieve these lower test times, the thermal chamber must be sealed from warm air leaks. For two different fan configurations, the test time can be cut in half.

Even though modeling was not an original task of this project a significant amount of time was spent on developing modeling techniques. Fluent models developed to determine the air flow path around a 155 mm shell. These models determined the best locations for fan placement within the thermal chamber. The enthalpy method, though not compared to actual test results, provided an insight into the problem of applying analysis to research. An model can be used to determine an optimum value for a variable. Often it is difficult to implement the optimum value into the actual system.

A project may not go as planned. A major component, out of your control, may go wrong. The project must still be finished. The goals can still be achieved if you keep working on it. This is what happened in our project. We had a budget crisis and could not build our redesigned thermal chamber. We had to test our ideas with thermal chamber that we felt was inadequate. After several attempts, we were able to significantly reduce the test time. We found ways to attach the thermocouples that did not involve welding. These attachment techniques resulted in accurate temperature measurements.

7.2 Preston Harris' Conclusions

The models done by both Preston and Sara, show the thermal chamber can be used to develop characteristic plots that can be used for identifying the test fluids within the shell. Although the models can not be confirmed, the feeling is confident that their predictions are close to the expected test results.

From the tests its apparent that whether using a thermocouple or a heat flux gage characteristic plots can be made for various chemicals. These characteristic plots could be used to identify a chemical within the shell.

8.0 Recommendations for Future Work

This project had two major goals. The first is to reduce the test below 2 hours. The second goal was to develop an appropriate thermocouple attachment technique. Even though these goals were achieved there are several areas where informative work can still be completed. These areas include construction of the redesigned thermal chamber and the corresponding testing, continuation of the modeling schemes developed during this phase of the project, and redesign of the recirculating cooler system for field use.

The thermal chamber has been redesigned to provide a higher heat transfer rate to the chemical munition shell. The higher rate should reduce the test time below the 2 hour limit. The redesigned thermal chamber is capable of performing induced air flow around the 155 mm shell. Test on the 155 mm shell and the 4.2 in mortar shell should be conducted in the future to verify that the 2 hour test time is satisfied. Additionally, the chamber ends can be modified to prevent warm air from entering the thermal chamber.

The models developed in this phase of the project will provide important information to future parts of the project. The enthalpy method can provide an estimate of the optimal convective heat transfer rate. The optimal convective heat transfer rate will provide an insight into fan sizing. Fluent modeling can be improved by including three dimensional models of the chamber with fans, inclusion of buoyancy terms in the air, and the phase change of water can be added to the heat transfer model. Tests could then be performed to confirm the models test time and heat flux across the shell. Possible redesign for field use may be considered.

9.0 References

Alexiades, V. and A. D. Solomon, *Mathematical Modeling of Melting and Freezing Processes*, Hemisphere
    Publishing Corp., Washington, DC, 1993.

ASTM Special Technical Publication 470B, *Manual on the Use of Thermocouples in Temperature Measurement*, American Society for Testing and Materials, Philadelphia, PA, 1987.

Ozisik, M. Necati, *Finite Difference Methods in Heat Transfer*, CRC Press, Boca Raton, 1994.

Appendix A: Project Management

A schedule was developed at the beginning of the project. The schedule was constrained to the three month time period of winter quarter. Due to the changes in the senior design class requirements, the project was given six months for completion. At this point, the schedule was revised to follow the six month period. Early into the fourth month, a funding problem was discovered. This halted all construction of the redesigned thermal chamber. It should be noted that if this problem had not been encountered the redesigned thermal chamber could have been built and optimized over the last two months of the project. During the optimization process extensive testing on the 155 mm and 4.2in mortar shells were scheduled. This period may have lent itself to exploring past test fluids.

The revised schedule is presented in figure 1. The construction and optimization of the redesigned thermal chamber stopped in early April when a budget crisis was encountered. Work continued on the development of appropriate models in Fluent, testing of the convection coefficient and data acquisition, and the enthalpy method model. Of course, because the redesigned thermal chamber has not been constructed it can not be optimized or test.

	Jan. 21	Jan. 24	Feb. 7	Mar. 14	Mar. 18	Mar. 28	Apr.14	Apr.28	May. 9	May.29
Preliminary Design Review	■									
Thermal Analysis of Thermal Chamber		■								
Testing of Convection Improvements			■	■	■	■	■	■		
Redesign and Material Selection			■	■	■	■		■		
Data Acquisition			■	■	■	■	■			
Enthalpy Method Model Development		■	■	■	■		■			
Concept Design Review						■				
Fluent Modeling Development							■			
Order Materials				■	■	■	■			
Construct Chamber								■		
Optimize Chamber								■		
Testing in New Thermal Chamber									■	
Final Report and Project Review										■

Figure 1. Project schedule

Budget:

The proposed equipment and materials budget was faxed to Dr. John Morrison at INEL on 1/6/97 is shown in table 1. This budget was approved. The project commenced with a total equipment and materials budget of $3020. The facilities and faculty supervision were provided by Utah State University. Student stipends totaling $3000.00 were requested separately.

Table 1. Project Budget

Expense	Amount Budgeted	Actual Spending
Thermal Chamber		
Walls	$ 500.00	$ 399.21
Insulation		
Mylar	$ 30.00	
2 Part Foam	$ 50.00	$ 70.00
End Closures	$ 50.00	
Exterior Chamber Support System	$ 40.00	
Shell Support System	$ 300.00	
Increasing Convection Coefficient	$ 150.00	$ 77.23
Temperature Measurement System		
Calibrate Datalogger	$ 100.00	$ 107.31
TC Stress Relievers	$ 50.00	
Miscellaneous		$ 192.13
Recirculating Cooler System		
Cooling Tubes	$ 1,000.00	
Heat Transfer Fluid	$ 250.00	
General Construction Materials	$ 500.00	$ 161.64
Total	$ 3,020.00	$ 1,007.52

Several funding difficulties were encountered in early April. This difficulties prevented the thermal chamber from being built and optimized. The money actually spent by the project is reported in table 1.

Team Member Tasks and Responsibilities:

At the onset of this project, the tasks and responsibilities were divided between the team member. The basis for this division of labor was the qualifications of each team member to perform the required duties.

Initially, Sara Gifford was responsible for the thermal analysis of the current recirculating cooler system, thermodynamic and heat transfer analysis throughout the

project, documentation of tests, and materials acquisition. Preston Harris' responsibilities were focused on data acquisition, chamber construction, increasing the convection heat transfer within the chamber, improving the thermocouple attachment technique, and communication with Dr. John Morrison at the INEL. Dr. J. Clair Batty's role was to periodically review the work, give advice, and secure the necessary funds for project completion.

Sara Gifford performed the complete thermodynamic analysis of the current recirculating cooler system. A thermal circuit was developed and analyzed to determine the areas most in need of improvement. The suggestion of Dr. John Morrison and Dr. Randy Clarksean that a low convection heat transfer rate through the air gap existed was verified. A simple numerical model employing the enthalpy method was developed with the advice of Dr. Spall. This model can be used to estimate the convection heat transfer coefficient produced by a fan. Each test was documented in Sara's logbook with a test setup description, a temperature time plot, and conclusions. Sara helped make material selection decisions. She calculated the potential heat transfer rate through a variety materials and thickness' to determine the appropriate interior wall material and thickness. Other specifications were made from her calculations including copper tube length and heat transfer fluid volume. Sara kept track of materials acquisition, though the materials were acquired primarily by Preston Harris. Sara completed her responsibilities in this project.

Preston Harris was responsible for selecting materials, building the thermal chamber, data acquisition increasing the convection heat transfer within the chamber, improving thermocouple attachment technique and communicating with Dr. John Morrison. Preston used Sara Gifford's heat analysis to determine desirable material properties for the thermal chamber. Preston then used selection criteria to narrow the choices. Preston, showed his results to Sara for confirmation. After approval, the materials were acquired. Halfway through the project funding problems occurred, building of the thermal chamber was stopped. When the funding stopped Preston used his time to start modeling the chamber using a commercially available computational fluid code dynamics, Fluent. The models were then used to evaluate the chamber. This modeling proved useful in evaluating placement of

the fans and other improvements. To increase the convection heat transfer coefficient, Preston researched fans and choose the size of the fans.

Preston analyzed test results of thermocouples. He also developed, and tested a procedure to safely mount the thermocouple to a live specimen.

Programs for data acquisition, the actual data acquisition and tests were setup by Preston.

Preston tried to brief Dr. Morrison on all significant details and decisions on the project.

Although the thermal chamber construction was halted Preston kept himself busy by shifting his work towards modeling. Over all Preston accomplished his duties in as far as it was possible.

Appendix B: Calculations

Interior Wall Specification:

Interior chamber wall must satisfy three criteria. The interior wall must be made of a material with a high coefficient of thermal conductivity to provide a high heat transfer rate inside the thermal chamber. The interior wall must not permanently deform when the shell is placed in the chamber. The cost of the material must also be considered. A study of potential materials was conducted. Copper and aluminum were the material choices most closely examined. These materials are relatively inexpensive, readily available, and easily formed into a tube.

The first criteria is the most important to be satisfied. If nothing else, the interior chamber wall must allow a high heat transfer rate. The maximum heat transfer rate occurs when the warm shell is inserted in the thermal chamber. The temperature difference is the maximum at this instant. The possible heat transfer rates can be calculated with the conduction expression. The heat transfer area is based on the inside diameter of the thermal chamber. The Δx is the thickness of material through which the heat must be transferred. Table 1 shows the heat transfer rates possible.

$$q = -kA \frac{\Delta T}{\Delta x}$$
$$\Delta T = 213K - 298K = -82$$
$$A = 2\pi rl = 2\pi(4")(48") = 0.6806m^2$$

Table 1. Possible heat transfer rates as a function of material and thickness.

Material	Thickness (in)	Conductivity (W/m²K)	Heat Transfer Rate (kW)
2024 T6 Aluminum	1/8	177	3111
	¼	177	1555
	¾	177	518
Copper	1/8	400	7031
	¼	400	3515
	¾	400	1171

The recirculating cooler can remove only 880W at -60°C. The heat removal capability can be compared with the maximum heat removal rates shown in table 1 to select the appropriate material and thickness. This comparison shows that all the potential materials and thickness' will not impede the heat transfer rate.

Aluminum was selected as interior chamber wall because it is less expensive and has a higher yield strength than copper.

Copper Tube Length Calculation:

The interior chamber wall is to be surrounded by a coil that delivers the cold heat transfer fluid to the thermal chamber. The coil is to made of copper tubing. Copper tubing is readily available in any hardware store. It is malleable. This allows it to be easily shaped into the coil. Most importantly, copper has a high coefficient of thermal conductivity. Conduction is the heat transfer mechanism to transfer heat from the thermal chamber to the heat transfer fluid. The copper tubing has one drawback. It is prone to kinks and permanent bends. FTS Systems sells Goodyear rubber tubing for $14 per foot. The tubing would be the first choice because it is flexible at room temperature, it is not subject to kinks and permanent bending. Copper is the least expensive tubing available with a majority of favorable characteristics. The drawback of copper tubing can be minimized by using the flexible hoses and protecting the coil ends near the thermal chamber.

In the original thermal chamber, the copper tube wraps were spaced approximately 2" apart. The heat transfer rate from the interior chamber wall to the heat transfer fluid is lower than if the coils were closely spaced. The maximum heat transfer rate will occur when the copper tube coil is as dense as possible.

The required copper tube length is dependent on the diameter as well as the length of the coil. From the coil spring back calculations, the copper tubing must be formed into a coil that has a 7 ¾" diameter. This diameter will ensure that coil will fit snugly against the 8" diameter interior wall providing good thermal contact. The coil run the full length of the thermal chamber (4'). The coil will be made of 5/8" diameter copper tubing. This diameter will mate well with the fixtures of the recirculating cooler. The circumference of the coil is 24.35" (C=2πr). Seventy-seven loops are required in the coil (L/D$_{tube}$ = 4'/(5/8")). A good estimate of the required tube length is for this coil is 156.2" (C * # loops).

Heat Transfer Fluid Volume:

The heat transfer fluid can be purchased from FTS systems under the trade name HT-30 in gallon increments. Each gallon of HT-30 costs $125. The high cost of HT-30 makes the accuracy of this calculation very important. Over predicting the required volume heat transfer fluid will result in a large avoidable unnecessary expense. Under prediction of the required volume will cost test time once the new thermal chamber is built.

Volume of HT-30 required to fill copper tubing coil:

$$V_{coil} = \frac{\pi}{4} d_{tubing}^2 L = \frac{\pi}{4} (5/8")^2 (156.2') = 0.333 ft^3 = 2.49 gal$$

Volume of HT-30 required to fill flexible hoses:

$$V_{fh} = \frac{\pi}{4} d_{fh}^2 L_{fh} = \frac{\pi}{4} (0.5")(6') = 0.00818 ft^3 = 0.0612 gal$$

Volume of HT-30 required to fill the recirculating cooler reservoir:

$$V_r = 5L = 1.32 gal$$

Total volume of HT-30 required:

$$V_{tot} = V_{coil} + V_{fh} + V_r = 2.49 gal + 0.0612 gal + 1.32 gal = 3.87 gal$$

Two gallons of HT-30 were purchased for the original recirculating cooler system. A small amount of the HT-30 was spilled during the building and leak test stage of the

system. It is estimated that at least 1 ¾ gallons of the fluid remains for use. Therefore, 3 gal of HT-30 must be purchased for use in the improved recirculating cooler system. This will leave 0.8 gal of HT-30 left over. This amount is not excessive because invariably some fluid will be lost in the leak testing stage of the system. Over time, some of the heat transfer fluid can evaporate. The HT-30 fluid that remains after the system is up and running will help ensure the system can be used for a long period of time.

Appendix C: Theory and Algorithm of the Enthalpy Method

In purely crystalline materials, the liquid to solid phase change takes place at a discrete temperature, T_m, and is associated with the latent heat of the material. This means that a discontinuous jump occurs in the enthalpy, H, versus temperature curve at the freezing point of purely crystalline substances. Figure 1 shows the enthalpy of a material as a function of temperature.
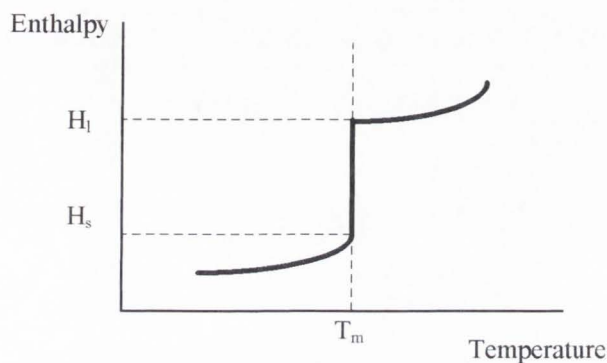

Figure 1. Enthalpy as a function of temperature for purely crystalline

The enthalpy (H) of a purely crystalline solid substance can be written as a set of equations for the liquid and solid phases.

$$H_l = C_p(T - T_m)$$
$$H_s = C_p(T - T_m) + L$$

Where C_p is the specific heat, T is the temperature, T_m is the freezing point of the substance, and L is the latent heat per unit mass. These equations can be solved for temperature as a function of enthalpy. The relationship between the enthalpy and the latent heat determines which equation applies:

$$T = T_m + \frac{H}{C_p}$$
$$T = T_m$$
$$T = T_m + \frac{H - L}{C_p}$$

The first equation represents the solid state (H<0). The second equation represents the phase change for which $0 \leq H \leq L$. The final equation represents the liquid phase (H>L).

The explicit enthalpy method will be specifically used to model the one dimensional solidification of the test fluid. This method is focused on the liquid to solid phase change that occurs at a discrete temperature. Initially, the liquid is at a uniform temperature, T_0, which is higher than the freezing point of the liquid, T_m. A boundary condition at the shell surface will be applied to model the convection heat transfer through the air gap. The boundary surface at x = 0 has a continuously decreasing temperature which is transferred from the interior chamber wall to the shell. This temperature must be less than freezing point temperature of the test fluid in order for it to change phases.

Two boundary conditions must be applied to model the phase change problem presented by the chemical weapons shell inside the thermal chamber. At the shell surface, the heat convected to the surface is equal to the heat conducted through the surface. This energy balance can be used to determine the temperature at node 1.

$$
E_{in} = E_{out}
$$
$$
h(T_i - T_\infty) = -k \frac{T_2 - T_1}{\Delta x}
$$
$$
T_i^{n+1} = \frac{hT_\infty - \frac{k}{\Delta x} T_2^n}{h - \frac{k}{\Delta x}}
$$

In this model, T_∞ set to -60°C the minimum temperature of the heat transfer fluid, h is the convective coefficient in W/m^2K induced by a fan, k is the coefficient of thermal conductivity of the steel shell (63.9 W/mK), T_1 is the temperature of node 1 on the surface of the shell, and T_2 is the temperature of node 2. The convective coefficient is assumed to remain constant throughout the test.

The second boundary condition is applied at centerline of the test fluid. At the centerline, a symmetric condition is applied. The symmetric condition is obtained from the problem geometry. The shell is modeled as one dimensional. In reality, it is a three dimensional entity. But the temperatures are assumed to be radially symmetric. The center of the test fluid is surrounded by uniform temperature. Therefore, the nodes on either side

of the centerline have the same temperature and enthalpy. This simplifies the enthalpy
equation for the centerline node, T_{cl}, to:

$$H_{cl}^{n+1} = H_{cl}^n + \frac{k}{\rho}\eta(2T_{cl-1}^n - 2T_{cl}^n)$$

where k is the coefficient of thermal conductivity in W/mK, ρ is the density of the test fluid,
T_i is temperature a the node specified in K and η is a stability condition. The temperature at
the centerline is determined by comparing the enthalpy to the latent heat and applying the
appropriate temperature equation.

The condition that should be satisfied for stability is dependent on the time step, the
node spacing, the material density, the specific heat, and thermal conductivity.

$$\eta = \frac{\Delta t}{(\Delta x)^2} < \frac{\rho C_p}{2k}$$

This equation can be solved for the time step. This is the equation by which the solution
progresses over time.

The general algorithm of the explicit enthalpy method can be followed to estimate
the time required for the test fluid to freeze. The convection coefficient induced by a fan
can be inferred by comparing a temperature time plot produced by the explicit enthalpy
method to one from an actual test. The general algorithm will be detailed as it is applied to
the phase change of a test fluid contained in a chemical munitions shell.

Initially, the temperatures and enthalpies must be known at each node. In the
chemical munitions shell tests, the entire shell is at room temperature (22°C). The enthalpy
can be calculated from the enthalpy liquid phase equation. This temperature corresponds to
the beginning of a test. This start of a test will be designated $t = 0$. The next time step is
specified with an n+1 subscript. It occurs Δt after the previous time step. The temperatures
and enthalpies at the next time step can be determined as follows:

a) Determine the temperature at the shell surface. The shell surface temperature is
   a dependent the convection coefficient of the air in the air gap, h, the conduction
   coefficient of the shell material, k, the interior chamber wall temperature, T_∞, and
   the distance between nodes, Δx.

$$T_1 = \frac{hT_\infty - \dfrac{k}{\Delta x}T_2}{h - \dfrac{k}{\Delta x}}$$

b) For each node 2 through M-1, calculate the enthalpy using the following equation:

$$H_i^{n+1} = H_i^n + \frac{k}{\rho}\eta\left(T_{i-1}^n - 2T_i^n + T_{i+1}^n\right)$$

where ρ is the density of the material, and $\eta = \Delta t/(\Delta x)^2$.

b) Use the appropriate value of H^{n+1} to determine the appropriate temperature equation to use to calculate the corresponding T^{n+1}.

c) Compute the centerline temperature by applying the boundary condition:

$$T_{M-1}^{n+1} = T_M^{n+1}$$

The explicit enthalpy method was implemented using FORTRAN. A copy of the program is included in the appendix.